



HAL
open science

Single-Molecule Magnet Behavior in Dy 3+ Half-Sandwich Complexes Based on Ene-Diamido and Cp* Ligands

J rome Long, Aleksei Tolpygin, Anton Cherkasov, Konstantin A. Lyssenko, Yannick Guari, Joulia Larionova, Alexander A. Trifonov

► To cite this version:

J rome Long, Aleksei Tolpygin, Anton Cherkasov, Konstantin A. Lyssenko, Yannick Guari, et al.. Single-Molecule Magnet Behavior in Dy 3+ Half-Sandwich Complexes Based on Ene-Diamido and Cp* Ligands. *Organometallics*, 2019, 38 (4), pp.748-752. <10.1021/acs.organomet.8b00901>. <hal-02047664>

HAL Id: hal-02047664

<https://hal.science/hal-02047664v1>

Submitted on 26 Nov 2020

HAL is a multi-disciplinary open access archive for the deposit and dissemination of scientific research documents, whether they are published or not. The documents may come from teaching and research institutions in France or abroad, or from public or private research centers.

L'archive ouverte pluridisciplinaire HAL, est destin e au d p t et   la diffusion de documents scientifiques de niveau recherche, publi s ou non,  manant des  tablissements d'enseignement et de recherche fran ais ou  trangers, des laboratoires publics ou priv s.



HAL Authorization

Single-Molecule Magnet Behavior in Dy³⁺ Half-Sandwich Complexes based on ene-diamido and Cp* Ligands.

Jérôme Long*,^a Aleksei O. Tolpygin,^b Anton V. Cherkasov,^b Konstantin A. Lyssenko,^c Yannick Guari,^a Joulia Larionova,^a Alexander A. Trifonov*,^{b,c}

^a Institut Charles Gerhardt, Equipe Ingénierie Moléculaire et Nano-Objets, Université de Montpellier, ENSCM, CNRS. Place Eugène Bataillon, 34095 (France).

^b Institute of Organometallic Chemistry of Russian Academy of Sciences, 49 Tropinina str., GSP-445, 630950, Nizhny Novgorod (Russia).

^c Institute of Organoelement Compounds of Russian Academy of Sciences, 28 Vavilova str., 119334, Moscow (Russia).

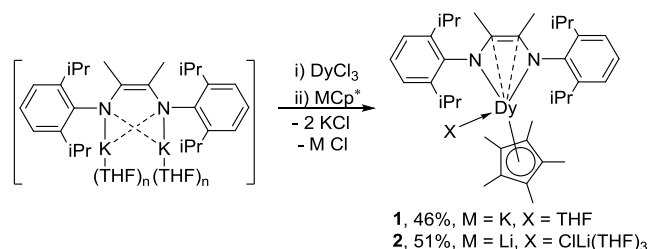
ABSTRACT: We report in this communication the synthesis, structure and magnetic investigations of two new half-sandwich complexes [Dy(DAD)Cp*(THF)] (**1**) and [Li(THF)₃][Dy(DAD)Cp*Cl] (**2**) (Cp* = C₅Me₅, DAD = [2,6-iPr₂C₆H₃N–CMe=CMe–NC₆H₃iPr₂-2,6]). Both compounds exhibit zero-field SMM behavior but distinct relaxation dynamics originating from difference in the arrangement of Cp* and DAD ligands. The anisotropic barrier for **1** is found one order of magnitude greater than for **2**.

Coordination complexes exhibiting slow relaxation of their magnetization associated with magnetic bistability show tremendous potentialities for information storage or spin-based computing.¹ Since the report of such effect more than two decades ago,² the chemical design and resulting properties of such Single-Molecule Magnets (SMMs) have been greatly enhanced by taking advantage of the fascinating properties of lanthanide ions.^{1b, 3} In 4f complexes, the appropriate combination between a specific lanthanide ion and surrounding ligands generates a crystal-field that may allow the appearance of an anisotropic barrier, Δ , that separates two opposite directions of the magnetic moment ($\pm m_j$). Naturally, increasing the crystal-field splitting should result in larger anisotropic barriers and blocking temperatures (which could be the temperature at which or relaxation time is equal to 100 s or alternatively as the highest temperature at which an hysteresis loop is observed).⁴ Such systems with largely separated $\pm m_j$ states could be engineered based on simple electrostatic considerations that exploit the optimum stabilization the electronic density of the 4f ions. Thus, lanthanide ions such as Dy³⁺ exhibiting oblate electronic density are efficiently stabilized by axial crystal-field that maximizes the splitting of the m_j levels and stabilizes the highest $m_j = \pm 15/2$ states, while minimizing the Quantum Tunneling of the Magnetization (QTM). However, such scenario is frequently altered by the existence of additional spin-lattice relaxation processes (Raman and direct) which create underbarrier relaxation paths.^{1b, 3, 5}

One possible strategy to obtain large axial crystal-field relies on the use of coordination⁶ or organometallic chemistry ligands⁷ that reduce the lanthanide coordination number while simultaneously

affording an efficient stabilization of the 4f electronic density. In this regards, major advances have been recently achieved with Dy³⁺ metallocenium complex based on cyclopentadienyl (Cp^R) ligands⁸ that show exceptional magnetic hysteresis features that could overcome liquid nitrogen's temperature.⁹ In this last example, the heteroleptic sandwich complex [Dy(Cp^{iPr5})(Cp*)][B(C₆F₅)₄] was found to exhibit large anisotropy thanks to a synergy between short Dy–Cp^{iPr5} distances and large Cp–Dy–Cp angle. Additionally, these impressive relaxation dynamics appear to be not solely related to the targeted coordination environment but also to the reduced molecular vibrations (metal-ligands vibrational modes) imposed by the rigid Cp ligands.^{5, 8a, 8b, 9} It appears therefore essential to gain deeper understanding on the parameters affecting such spin-phonon coupling.

In this sense, we have recently reported the use of doubly reduced diazabutadiene ligands for the design of lanthanide SMMs.¹⁰ These anionic ligands, acting as both, n and π -electron donors, benefit from a large steric and electronic tunability that could be taken as an advantage to create highly axial crystal-field. In our previous studies, the homoleptic Li(DME)₃[Dy(DAD)₂] complex (DAD = [2,6-iPr₂C₆H₃N–CH=CH–NC₆H₃iPr₂-2,6]) exhibit a genuine SMM behaviour.^{10b} Yet, despite a significant crystal-field splitting generated by these ligands, Raman relaxation was found to dominate the relaxation dynamics. Aiming at reducing this spin-phonon coupling while increasing the magnetic anisotropy, we propose here to associate bulky DAD-type ligands, that are known to generate short Dy–N distances, with rigid Cp* moiety in order to design heteroleptic half-sandwich dysprosium complexes.



Scheme 1: Synthesis of **1** and **2**.

The synthetic strategy to design the targeted heteroleptic half-sandwich-type complexes $[\text{Dy}(\text{DAD})\text{Cp}^*]$ relies on the cascade of reactions of anhydrous DyCl_3 with $[\text{DADK}_2(\text{THF})_n]$ and alkali metal cyclopentadienide MCp^* ($\text{M} = \text{Li}, \text{K}$) (Scheme 1). Using KCp^* leads to the formation of a salt-free complex $[\text{Dy}(\text{DAD})\text{Cp}^*(\text{THF})]$ (**1**), while in the case of LiCp^* , ate-complex $[\text{Li}(\text{THF})_3(\mu^2\text{-Cl})\text{Dy}(\text{DAD})\text{Cp}^*]$ (**2**) was isolated (see ESI for details).

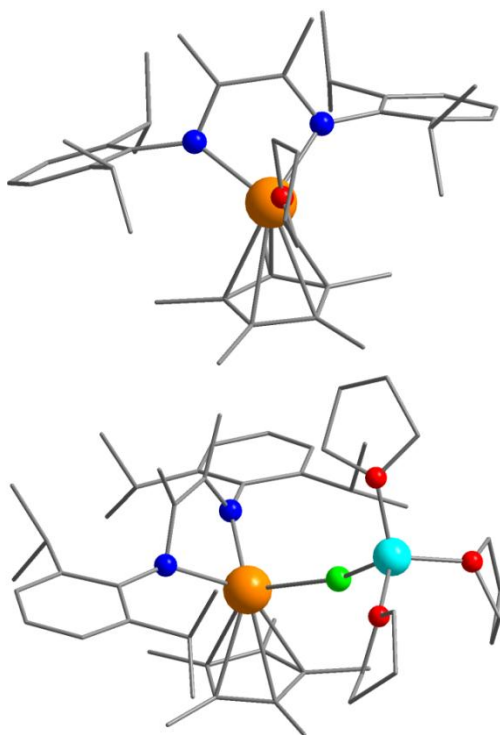


Fig. 1. Structure of **1** (top) and **2** (bottom). Color code: orange, Dy; red, O; grey, C; green, Cl; light blue, Li. Hydrogen atoms have been omitted for clarity.

The X-ray diffraction studies indicate that both compounds crystallize in the $P2_1/c$ space group with a unique complex within the asymmetric unit (Table S1). Compound **1** is isostructural to the ytterbium complex we recently obtained.¹¹ The coordination environments of the Dy^{3+} in **1** and **2** are composed of one Cp^* ligand, one dianionic $2\sigma:\eta^2$ ene-diamido DAD^{2-} ligand and one coordinated THF molecule (for **1**) or $\mu^2\text{-ClLi}(\text{THF})_3$ fragment (for **2**). The Dy- C_{Cp} bond lengths in **1** are ranging from 2.612(2) to 2.727(1) Å, the Dy- C_{Cenr} distance is of 2.391(2) Å (Table S2). The Dy-N bond lengths are slightly different and equal to 2.189(2) and 2.202(2) Å. With respect to **1**, the Dy- C_{Cenr} distance in **2** (2.367(2) Å) is slightly shorter, while one Dy-N bond length is longer (2.198(2) and 2.205(2) Å). The Dy-N bond lengths in **1** and **2** are noticeably shorter than the related values measured for eight-coordinate Dy^{3+} complexes and correspond to covalent Dy-N bonds.¹² The short distances between the Dy^{3+} ions and the carbon atoms of the NCCN moiety in **1** (2.837(2), 2.845(2) Å) and **2** (2.764(2), 2.769(2) Å) are indicative of η^2 -coordination of the C=C bonds to the Dy^{3+} ion. However, these distances are longer than in the previously reported $[\text{Li}(\text{DME})_3][\text{Dy}(\text{DAD})_2]$ (2.672(3)–2.712(5) Å).^{10b} The Dy-O distance in **1** is equal to 2.362(2) Å. In **2**, the Cl^- ligand μ^2 -bridges $[\text{Li}(\text{THF})_3]^+$ and Dy^{3+} ions. The Dy-Cl distance is 2.6403(6) Å and the Li-Cl one is of 2.339(4) Å. Taking into account the two centroids defined by the DAD^{2-} (NCCN) and Cp^* ligands, bite angles of 142.0(2)° and 139.6(2)° are found for **1** and **2** respectively. The shortest intermolecular $\text{Dy}^{3+}\text{-Dy}^{3+}$ distance measured

in **1** (9.543(2) Å) proved to be noticeably shorter compared to that in **2** (11.413(2) Å) (Fig. S1).

The magnetic properties of **1** and **2** were investigated in both, static and dynamic modes. The detailed dc measurements could be found in the ESI and reveal differences that may originate from dissimilar crystal-field splitting.

The occurrence of slow relaxation of the magnetization was investigated by alternating current (ac) measurements. Under a zero-dc field, the compounds exhibit a clear frequency dependence in the in-phase (χ') and in the out-of-phase (χ'') components of the magnetic susceptibility (Fig. 2, Fig. S4-S5) indicating a SMM behavior. While for **1** a maximum could be discerned, **2** exhibits a very broad signal without a clear maximum of χ'' . The Cole-Cole plots (Fig. S6) reveal the presence of two relaxation processes for **1**. These data could be fitted with the sum of two modified Debye functions¹³ for **1** (Table S3) leading to large values (*i.e.* 0.6) of the α parameter at low temperature for the main relaxation process but such treatment yields to unrealistic fitting parameters for **2**.

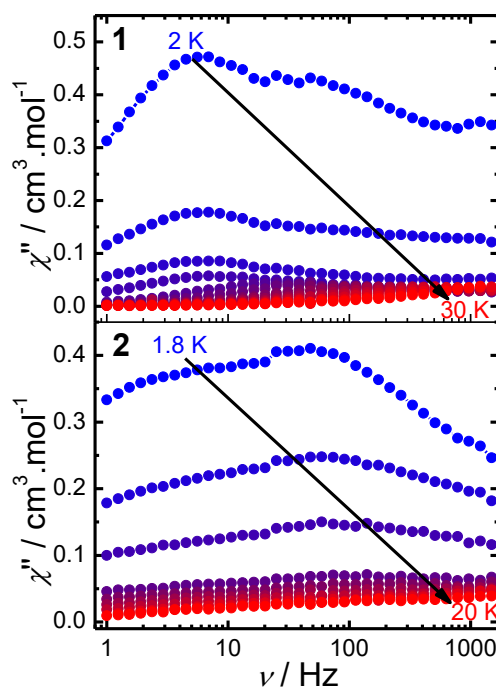


Fig. 2. Frequency dependence of the out-of phase (χ'') susceptibilities for **1** and **2** under a zero dc-field.

Insights into the dynamics of the relaxation of the magnetization could be obtained from the temperature dependence of the relaxation time, τ . The broad maximum for **2** prevent extracting relevant values of τ . The $\ln \tau$ vs. T^{-1} plot for **1** related to the main relaxation process deviates from the linearity before becoming temperature independent at low temperature, indicating the presence of QTM (Fig. 3, Fig. S7). Consequently, the overall data range could be modeled using the following equation: $\tau^{-1} = \tau_0^{-1} \exp(-\Delta/kT) + CT^n + \tau_{\text{QTM}}^{-1}$ (Eq. 1).¹⁴ The first term accounts for a thermally activated process, while the second and third ones stand for two-phonon Raman and QTM, respectively. In order to avoid over-parameterization, n was fixed to different values until getting the best fitting coefficient. The obtained fit parameters (Table 1) point out that a relaxation involving these three different processes. The low value of the n exponent as observed in others Dy/Cp systems^{8a, 8b, 9} may indicate the presence of optical phonons¹⁵

Table 1: Fit parameters of the temperature dependence of the relaxation time for **1** and **2**.

Compound	Δ (cm^{-1})	τ_0 (s)	n^*	C ($\text{s}^{-1}\cdot\text{K}^{-m}$)	A ($\text{s}^{-1}\cdot\text{K}^{-l}$)
1 (0 Oe)	254 ± 17	$(6 \pm 5) \times 10^{-10}$	3	0.008 ± 0.005	-
1 (2000 Oe)	206 ± 10	$(10 \pm 4) \times 10^{-9}$	3	0.007 ± 0.003	-
2 (1000 Oe)	20 ± 4	$(5 \pm 3) \times 10^{-9}$	-	-	281 ± 139

*fixed parameter

In order to reduce the observed QTM, the field dependence of the ac susceptibilities was studied. An increase of the relaxation time is observed with optimum fields found at 2000 and 1000 Oe for **1** (15 K) and **2** (2 K), respectively (Fig. S8). The field dependence of τ could be modeled with the equation $\tau^{-1} = DH^4T + B_1/(1+B_2H^2) + K$ (Eq. 2), for which the first term accounts for the direct process (for Kramers-ion), the second one for the QTM and the K constant accounts for the field-independent Raman and thermally activated processes (Fig. S9, Table S4). The frequency dependence of the ac susceptibilities measured under these dc fields confirms the shortcut of the QTM. While a broad maximum of χ'' could be still observed for **1**, applying a dc field totally modifies the frequency dependence of χ'' for **2** (Fig. S10). Thus, although a plateau is observed at low frequencies (also confirmed by the Cole-Cole plots, Fig. S11, Table S6), a clear maximum could be now discerned allowing the extraction of the relaxation time. The temperature dependence of the relaxation time (Fig. 3) for both complexes could be fitted with: $\tau^{-1} = \tau_0^{-1}\exp(-\Delta/kT) + CT^n + AT$ (Eq. 3) (Fig. 3, Fig. S7, Table 1) in which the third term accounts for the direct process. Δ is found one order of magnitude lower for **2** with respect to **1** confirming an important difference in the crystal-field splitting as previously evidenced from the dc measurements. Moreover, although no direct process could be evidenced for **1**, it contributes greatly to the overall relaxation for **2**, while the Raman process is found inoperative;

The magnetic analysis indicates a dramatic variation in the dynamic of slow relaxation of the magnetization for **1** and **2** despite a closely related structure. To get further insights, magneto-structural correlations could be achieved by evaluation of the orientation of the anisotropic axes of the ground Kramers doublet using the MAGELLAN¹⁶ software based on electrostatic considerations. As expected, the orientation of the anisotropic axes for both complexes are mainly imposed by both, Cp* and DAD-Me ligands (Fig. S12). Hence, a deviation of less than 15° with the anisotropic axis is observed between the centroids of DAD-Me and Cp* ligands (Table S7). Moreover, the THF or chloride in **1** and **2**, respectively, define a mean angle close to 90° with the anisotropic axis, inducing a transverse component that explains the QTM. Surprisingly, substitution of a THF by a negatively charged chloride does not induce a significant tilt of the anisotropic axis for **2**. This could be imputed to the rather long Dy-Cl distance of 2.640 Å to compare with the shorter Dy-O one of 2.363 Å, counterbalancing the effect of the chloride negative charge. On the other hand, **1** exhibits the shortest Dy³⁺-Dy³⁺ distance. It should therefore exhibit the highest tunneling rate caused by dipolar interactions which is not experimentally observed.

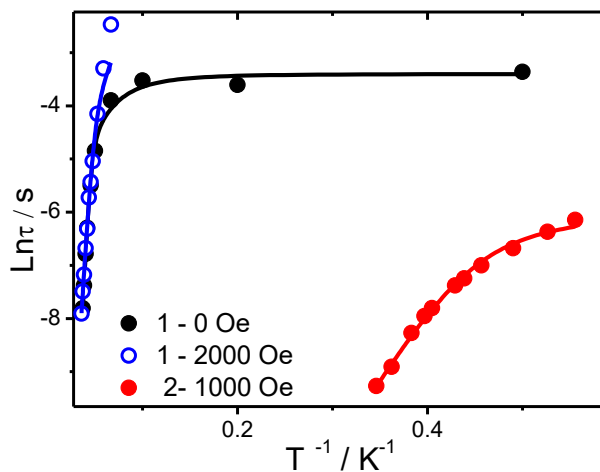


Fig. 3. Temperature dependence of τ , for **1** and **2**. The solid lines correspond to the fit with Eq. 1 or Eq. 3.

Hence, the observed differences in the magnetic properties may be rather explained by subtle differences in the arrangement of DAD-Me and Cp* ligands. Recent studies on dysprosium metallocene complexes $[\text{Dy}(\text{Cp}^R)_2]^+$ clearly point out two critical parameters that affect the magnetic axiality in these systems: the Cp-Dy-Cp angle and Dy-C distances. Maximizing the anisotropy requires achieving large bite angles, while shortening the Dy-C bonds.¹⁷⁻²⁰ Despite the fact that the Dy-C are found slightly shorter in **2**, the greater bite angle Cp*-Dy-DAD associated with the reduced Dy-N distances for **1** may explain its larger crystal-field splitting and greater anisotropic barrier. Such dominant influence of the DAD ligand is also in line with its two-fold greater negative charge carried in comparison with Cp*.

Furthermore, the magnetic properties of **1** may be favorably compared with those obtained in our previously reported homoleptic complex $[\text{Li}(\text{DME})_3][\text{Ln}(\text{DAD})_2]$.^{10b} In this latter, the DAD-Dy-DAD angle was closer to the linearity (172°), but significantly larger Dy-N distances of 2.221-2.246 Å were found. In addition, the magnetization was found to mainly relax through a Raman process. Consequently, incorporation of rigid Cp* moieties in association with DAD ligands permits to increase the axiality while reducing the Raman relaxation.

In summary, we have reported in this article two different heteroleptic Dy³⁺ complexes based on DAD and Cp* ligands. Although they differ by the nature of an additional coordinated species (THF vs. Cl⁻), both compounds exhibit distinct slow relaxation of the magnetization dynamics caused by slight changes in the Dy-N distances and Cp*-Dy-DAD angles. Thanks to the great tunability of both, DAD and Cp ligands, extension to other heteroleptic complexes exhibiting shorter Dy-N distances and greater bite angles may be viewed as a promising route to enhance the magnetic relaxation properties in lanthanide SMM.

ASSOCIATED CONTENT

Supporting Information

The Supporting Information is available free of charge on the ACS Publications website. Experimental procedures, additional structural and magnetic data could be found in the PDF.

AUTHOR INFORMATION

Corresponding Author

*E-mail: jerome.long@umontpellier.fr

*E-mail: trif@iomc.ras.ru

Author Contributions

†All the authors contributed equally.

Notes

The authors declare no competing financial interests.

ACKNOWLEDGMENT

The financial support of the Russian Science Foundation is highly acknowledged (Project № 17-73-30036). The X-ray study of **1** has been carried out in the framework of the Russian state assignment (Theme № 44.2, Reg. № AAAA-A16-116122110053-1) using the equipment of The Analytical Center of IOMC RAS. The French authors thank the University of Montpellier, CNRS and PAC of ICGM.

REFERENCES

- (1) (a) Luzon, J.; Sessoli, R., Lanthanides in molecular magnetism: so fascinating, so challenging. *Dalton Trans.* **2012**, 41 (44), 13556-13567; (b) Woodruff, D. N.; Wippeny, R. E. P.; Layfield, R. A., Lanthanide single-molecule magnets. *Chem. Rev.* **2013**, 113 (7), 5110-5148; (c) Troiani, F.; Affronte, M., Molecular spins for quantum information technologies. *Chem. Soc. Rev.* **2011**, 40 (6), 3119-3129; (d) Bogani, L.; Wernsdorfer, W., Molecular spintronics using single-molecule magnets. *Nat. Mater.* **2008**, 7 (3), 179-186.
- (2) (a) Sessoli, R.; Tsai, H. L.; Schake, A. R.; Wang, S.; Vincent, J. B.; Foltling, K.; Gatteschi, D.; Christou, G.; Hendrickson, D. N., High-spin molecules: [Mn12O12(O2CR)16(H2O)4]. *J. Am. Chem. Soc.* **1993**, 115 (5), 1804-1816; (b) Sessoli, R.; Gatteschi, D.; Caneschi, A.; Novak, M. A., Magnetic bistability in a metal-ion cluster. *Nature* **1993**, 365, 141.
- (3) (a) Tang, J.; Zhang, P., Lanthanide Single-Ion Molecular Magnets. In *Lanthanide Single Molecule Magnets*, Springer Berlin Heidelberg: Berlin, Heidelberg, 2015; pp 41-90; (b) Layfield, R. A.; Murugesu, M., *Lanthanides and Actinides in Molecular Magnetism*. Wiley: 2015; (c) Ungur, L.; Chibotaru, L. F., Strategies toward High-Temperature Lanthanide-Based Single-Molecule Magnets. *Inorg. Chem.* **2016**, 55 (20), 10043-10056.
- (4) Gatteschi, D.; Sessoli, R.; Villain, J., *Molecular Nanomagnets*. Oxford Univ. Press, New York, 2007 **2006**.
- (5) Escalera-Moreno, L.; Baldoví, J. J.; Gaita-Ariño, A.; Coronado, E., Spin states, vibrations and spin relaxation in molecular nanomagnets and spin qubits: a critical perspective. *Chem. Sci.* **2018**, 9 (13), 3265-3275.
- (6) (a) Gupta, S. K.; Rajeshkumar, T.; Rajaraman, G.; Murugavel, R., An air-stable Dy(III) single-ion magnet with high anisotropy barrier and blocking temperature. *Chem. Sci.* **2016**, 7 (8), 5181-5191; (b) Chen, Y.-C.; Liu, J.-L.; Ungur, L.; Liu, J.; Li, Q.-W.; Wang, L.-F.; Ni, Z.-P.; Chibotaru, L. F.; Chen, X.-M.; Tong, M.-L., Symmetry-Supported Magnetic Blocking at 20 K in Pentagonal Bipyramidal Dy(III) Single-Ion Magnets. *J. Am. Chem. Soc.* **2016**, 138 (8), 2829-2837.
- (7) (a) Layfield, R. A., Organometallic Single-Molecule Magnets. *Organometallics* **2014**, 33 (5), 1084-1099; (b) Liu, J.; Chen, Y.-C.; Liu, J.-L.; Vieru, V.; Ungur, L.; Jia, J.-H.; Chibotaru, L. F.; Lan, Y.; Wernsdorfer, W.; Gao, S.; Chen, X.-M.; Tong, M.-L., A Stable Pentagonal Bipyramidal Dy(III) Single-Ion Magnet with a Record Magnetization Reversal Barrier over 1000 K. *J. Am. Chem. Soc.* **2016**, 138 (16), 5441-5450; (c) Gregson, M.; Chilton, N. F.; Ariciu, A.-M.; Tuna, F.; Crowe, I. F.; Lewis, W.; Blake, A. J.; Collison, D.; McInnes, E. J. L.; Wippeny, R. E. P.; Liddle, S. T., A monometallic lanthanide bis(methanediide) single molecule magnet with a large energy barrier and complex spin relaxation

behaviour. *Chem. Sci.* **2016**, 7 (1), 155-165; (d) Ding, Y.-S.; Chilton, N. F.; Wippeny, R. E. P.; Zheng, Y.-Z., On Approaching the Limit of Molecular Magnetic Anisotropy: A Near-Perfect Pentagonal Bipyramidal Dysprosium(III) Single-Molecule Magnet. *Angew. Chem. Int. Edit.* **2016**, 55 (52), 16071-16074; (e) Meng, Y.-S.; Xu, L.; Xiong, J.; Yuan, Q.; Liu, T.; Wang, B.-W.; Gao, S., Low-Coordinate Single-Ion Magnets by Intercalation of Lanthanides into a Phenol Matrix. *Angew. Chem. Int. Edit.* **2018**, 57 (17), 4673-4676; (f) Day, B. M.; Guo, F.-S.; Layfield, R. A., Cyclopentadienyl Ligands in Lanthanide Single-Molecule Magnets: One Ring To Rule Them All? *Acc. Chem. Res.* **2018**, 51 (8), 1880-1889.

(8) (a) Guo, F.-S.; Day, B. M.; Chen, Y.-C.; Tong, M.-L.; Mansikkamäki, A.; Layfield, R. A., A Dysprosium Metallocene Single-Molecule Magnet Functioning at the Axial Limit. *Angew. Chem. Int. Edit.* **2017**, 56 (38), 11445-11449; (b) Goodwin, C. A. P.; Ortu, F.; Reta, D.; Chilton, N. F.; Mills, D. P., Molecular magnetic hysteresis at 60 kelvin in dysprosium(III). *Nature* **2017**, 548 (7668), 439-442; (c) Randall McClain, K.; Gould, C. A.; Chakarawet, K.; Teat, S. J.; Groshens, T. J.; Long, J. R.; Harvey, B. G., High-temperature magnetic blocking and magneto-structural correlations in a series of dysprosium(III) metallocene single-molecule magnets. *Chem. Sci.* **2018**, 9 (45), 8492-8503.

(9) Guo, F.-S.; Day, B. M.; Chen, Y.-C.; Tong, M.-L.; Mansikkamäki, A.; Layfield, R. A., Magnetic hysteresis up to 80 kelvin in a dysprosium metallocene single-molecule magnet. *Science* **2018**, 362 (6421), 1400-1403.

(10) (a) Trifonov, A. A.; Shestakov, B.; Long, J.; Lyssenko, K.; Guari, Y.; Larionova, J., An Organoytterbium(III) Complex Exhibiting Field-Induced Single-Ion-Magnet Behavior. *Inorg. Chem.* **2015**, 54 (16), 7667-7669; (b) Long, J.; Shestakov, B. G.; Liu, D.; Chibotaru, L.; Guari, Y.; Cherkasov, A.; Fukin, G. K.; Trifonov, A.; Larionova, J., An organolanthanide(III) single-molecule magnet with an axial crystal-field: influence of the Raman process over the slow relaxation. *Chem. Commun.* **2017**, 53, 4706-4709.

(11) Selikhov, A. N.; Mahrova, T. V.; Cherkasov, A. V.; Fukin, G. K.; Larionova, J.; Long, J.; Trifonov, A. A., Base-Free Lanthanoidocenes(II) Coordinated by Bulky Pentabenzylcyclopentadienyl Ligands. *Organometallics* **2015**, 34 (10), 1991-1999.

(12) (a) Zhang, X.-Q.; Lin, M.-S.; Hu, B.; Chen, W.-Q.; Zheng, L.-N.; Wu, J.; Chen, Y.-M.; Zhou, F.-Y.; Li, Y.-H.; Li, W., Anionic lanthanide complexes supported by a pyrrole-based tetradentate Schiff base ligand: Synthesis, structures and catalytic activity toward the polymerization of ϵ -caprolactone. *Polyhedron* **2012**, 33 (1), 273-279; (b) Williams, U. J.; Mahoney, B. D.; DeGregorio, P. T.; Carroll, P. J.; Nakamaru-Ogiso, E.; Kikkawa, J. M.; Schelter, E. J., A comparison of the effects of symmetry and magnetoanisotropy on paramagnetic relaxation in related dysprosium single ion magnets. *Chem. Commun.* **2012**, 48 (45), 5593-5595.

(13) Guo, Y.-N.; Xu, G.-F.; Guo, Y.; Tang, J., Relaxation dynamics of dysprosium(III) single molecule magnets. *Dalton Trans.* **2011**, 40 (39), 9953-9963.

(14) Meihaus, K. R.; Minasian, S. G.; Lukens, W. W.; Kozimor, S. A.; Shuh, D. K.; Tylliszczak, T.; Long, J. R., Influence of pyrazolate vs N-heterocyclic carbene ligands on the slow magnetic relaxation of homoleptic trischelate lanthanide(III) and uranium(III) complexes. *J. Am. Chem. Soc.* **2014**, 136 (16), 6056-6068.

(15) Shrivastava, K. N., Theory of Spin-Lattice Relaxation. *physica status solidi (b)* **1983**, 117 (2), 437-458.

(16) Chilton, N. F.; Collison, D.; McInnes, E. J. L.; Wippeny, R. E. P.; Soncini, A., An electrostatic model for the determination of magnetic anisotropy in dysprosium complexes. *Nat. Commun.* **2013**, 4, 2551.

Single-Molecule Magnet in Dy³⁺ Half-Sandwich complexes

